Modeling of incident particle energy distribution in plasma immersion ion implantation

X. B. Tian, D. T. K. Kwok, and Paul. K. Chu[a)]
Department of Physics and Materials Science, City University of Hong Kong, 83, Tat Chee Avenue, Kowloon, Hong Kong

(Received 23 May 2000; accepted for publication 23 August 2000)

Plasma immersion ion implantation is an effective surface modification technique. Unlike conventional beam-line ion implantation, it features ion acceleration/implantation through a plasma sheath in a pulsed mode and non-line-of-sight operation. Consequently, the shape of the sample voltage pulse, especially the finite rise time due to capacitance effects of the hardware, has a large influence on the energy spectra of the incident ions. In this article, we present a simple and effective analytical model to predict and calculate the energy distribution of the incident ions. The validity of the model is corroborated experimentally. Our results indicate that the ion energy distribution is determined by the ratio of the total pulse duration to the sample voltage rise time but independent of the plasma composition, ion species, and implantation voltage, subsequently leading to the simple analytical expressions. The ion energy spectrum has basically two superimposed components, a high-energy one for the majority of the ions implanted during the plateau region of the voltage pulse as well as a low-energy one encompassing ions implanted during the finite rise time of the voltage pulses. The lowest-energy component is attributed to a small initial expanding sheath obeying the Child-Langmuir law. Our model can also deal with broadening of the energy spectra due to molecular ions such as N_2^+ or O_2^+, in which case each implanted atom only carries a fraction (in this case, half) of the total acceleration energy. © *2000 American Institute of Physics.*
[S0021-8979(00)00323-6]

I. INTRODUCTION

The use of ion implantation to enhance the surface properties of materials is well documented.[1,2] Conventional beam-line ion implantation is, however, inherently limited by its line-of-sight nature, and so direct application to components possessing irregular geometries is difficult. In comparison, plasma immersion ion implantation (PIII) (Refs. 3 and 4) features non-line-of-sight operation and obviates the need for complex sample manipulation. In PIII, the incident ion current density obeys the Child–Langmuir law, and implantation commences as soon as a negative voltage is applied to the sample. The experiment is usually conducted in a pulsed mode, and the rise and fall times of the sample voltage pulse are nonzero in real electrical circuits. Thus, ions with different energies are implanted into the biased surfaces. The rise time of the voltage pulse has a particularly large effect on this nonideal ion energy distribution and reduces the mean projected range of the ions. In many PIII applications, particularly semiconductor-related applications, the implantation depth must be well controlled, and it is thus critical to predetermine the energy distribution for more efficient determination of the appropriate processing protocols.

Various analytical and numerical models have been developed to determine the time-varying implantation current, total dose, and energy distribution of the implanted ions.[5–10] As far as the voltage rise time is concerned, several people, including Speth,[11] Stewart,[12] and Qin[13] have conducted investigations. In this work, we extend the work of Stewart[12] and derive an analytical model to predict the ion energy distributions. The proposed model features simple, easy to use analytical expressions to derive the energy spectra of the incident particles.

II. VOLTAGE/CURRENT WAVE-FORM AND ENERGY DISTRIBUTION

Figure 1 shows a schematic of the circuit of our PIII pulsed power supply in the City University of Hong Kong.[14] The high-voltage tetrode tube used in our modulator is not an ideal switch, and to make things worse, the pulse voltage shape is degraded by the capacitance of the cable, vacuum chamber, and plasma. Consequently, the typical rise and fall times of the pulse voltage/current resemble the experimental wave forms depicted in Fig. 2 as recorded by a capacitance divider (Pearson model 305A) and Rogowski coil (Pearson model 110) and a digital oscillator (Tektronix TDS360). The rise time t_r and fall time t_f of the implantation voltage pulse are determined by the resistance–capacitance (RC) constant of the circuit:[15]

$$t_r = R_{\mathrm{series}} \times (C_{\mathrm{cable}} + C_{\mathrm{chamber}} + C_{\mathrm{plasma}}), \quad (1)$$

$$t_f = (R_{\mathrm{pulldown}} \| R_{\mathrm{plasma}}) \times (C_{\mathrm{cable}} + C_{\mathrm{chamber}} + C_{\mathrm{plasma}}). \quad (2)$$

The oscillations in the current wave form demonstrate that the plasma is not a linear load to the modulator. As shown in Fig. 2, the current wave form can be divided into three zones.[16] The first or initial stage features a high instanta-

[a)]Author to whom correspondence should be addressed; electronic mail: paul.chu@cityu.edu.hk

 © 2000 American Institute of Physics

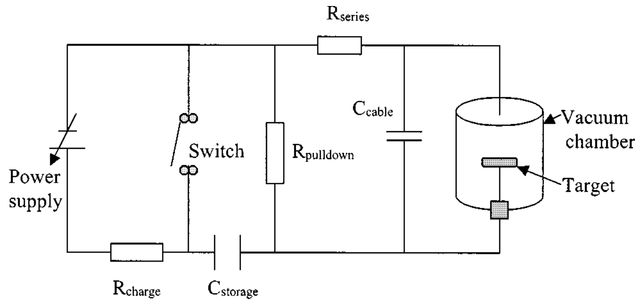

FIG. 1. Schematic of the electrical circuit of the City University of Hong Kong PIII modulator.

neous current induced by the plasma implantation and the capacitance effects of the high-voltage coaxial cable. In the second stage, the implantation current gradually decreases until the end of the voltage pulse. After the pulse is turned off (the fall-time stage), the implantation current decreases precipitously. Due to the small current, the last stage has a negligible effect on the final implantation results. Hence, in most applications, we can conveniently ignore the fall time in our calculation of the ion energy spectra.

A. Sheath expansion

To simulate the plasma sheath dynamics and resulting ion energy distribution, we assume that the applied voltage has a trapezoidal wave form as displayed in Fig. 2, and the plasma sheath expands in accordance with the quasistatic Child–Langmuir law under collisionless, cold plasma conditions. The Child law current density j_i for a voltage V across a sheath of thickness s is[8,12]

$$j_i = \tfrac{4}{9}\varepsilon_0 (2e/M)^{1/2} V^{3/2}/s^2, \tag{3}$$

where ε_0 is the free-space permittivity, and e and M are the ion charge and mass, respectively. Equating j_i to the charge per unit time crossing the sheath boundary,

$$en_i \frac{ds}{dt} = j_i \tag{4}$$

and

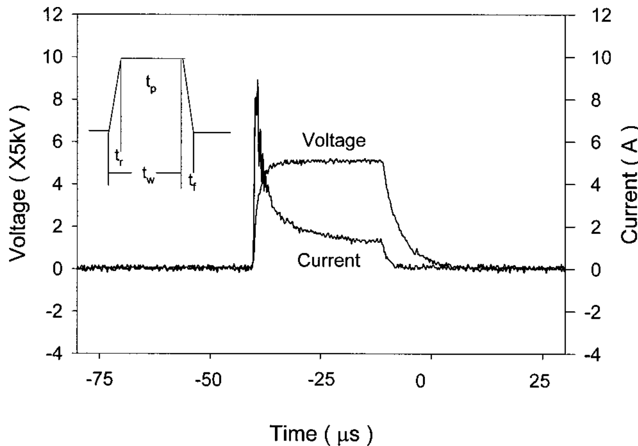

FIG. 2. Experimental current and voltage traces of a typical PIII process showing the three stages.

$$\frac{ds}{dt} = \frac{4}{9}\varepsilon_0 (2/en_i^2 M)^{1/2} V^{3/2}/s^2. \tag{5}$$

Integrating Eq. (5) from 0 to t_r (rise time) and from t_r to t_w (the entire pulse duration), we obtain

$$s_1 = \left(\frac{4}{15}\right)^{1/3} s_0 \omega_{pi}{}^{4/3} t_r^{-1/2} t^{5/6}, \quad \text{for } 0<t<t_r, \tag{6}$$

$$s_2 = \left(\frac{2}{3}\right)^{1/3} s_0 \omega_{pi}{}^{4/3} (t-0.6t_r)^{1/3}, \quad \text{for } t_r<t \tag{7}$$

where $S_0 = (2\varepsilon_0 V_0/en_0)^{1/2}$, and S_1 and S_2 are the dynamic sheath thicknesss during the rise time and plateau, respectively.

B. Energy spectra of incident ions

We assume that the ions once entering the plasma sheath are completely accelerated by the applied voltage. Thus, the ions implanted before the end of the rise time possess energies less than eV_0 and during the voltage plateau (steady state), the ions receive the full acceleration energy eV_0. The energy spectra, according to Eqs. (6) and (7), can be described as

$$\delta_{i,W_1,W_2} = 0.7368 \times (W_2{}^{5/6} - W_1{}^{5/6}) \times (x-0.6)^{-1/3} \quad (W_1 \leqslant W_2 < eV_0), \tag{8}$$

$$\delta_{eV_0} = 1 - 0.7368 \times (x-0.6)^{-1/3} \quad (W = eV_0), \tag{9}$$

where δ_{i,W_1,W_2} represents the fraction of the ions with energy between W_1 and W_2, δ_{eV_0} is the fraction of the ions with energy of eV_0, $x = t_w/t_r$, $W_1 = V_1/V_0$, and $W_2 = V_2/V_0$.

If $W_1 = 0$, Eq. (8) can be simplified to be

$$\delta_{i,W_2} = 0.7368 \times W_2{}^{5/6} \times (x-0.6)^{-1/3}, \tag{10}$$

where δ_{i,W_2} represents the number fraction of the ions with energy less than W_2. This is the same as Eq. (47) in Ref. 12 when the fall time is equal to zero:

$$\delta = \left(\frac{4}{15}\right)^{1/3} \times \frac{T_r{}^{1/3} \times (W_{\min}/V_0)^{5/6}}{S_t} + 1 - \left(1 - \frac{4}{15} \times \frac{T_f \times (W_{\min}/V_0)^{5/6}}{S_t{}^3}\right)^{1/3}, \tag{11}$$

where $T_r = \omega_{pi} t_r$, $T_f = \omega_{pi} t_f$, $S_t = s/s_0$, and t_f is the fall time.[12]

The correlation indicates that our assumption and approximation adopted in this model are proper.

C. Average energy of incident ions

In a single-voltage pulse, the energy imparted to the target W is the sum of the energy during the rise time W_1 and steady-state (plateau) W_2:

$$W_1 = \int_0^{t_r} en_i \frac{ds}{dt} \frac{t}{t_r} V_0 dt, \tag{12}$$

$$W_2 = e n_i V_0 (s_{t_w} - s_{t_r}). \tag{13}$$

Consequently,

$$\psi/V_0 = 1 - 0.4019 \times (x - 0.6)^{-1/3}, \tag{14}$$

where $e\psi$ is the average incident ion energy.

D. Energy distribution of implanted particles

The plasma in a typical PIII experiment consists of multiple species, for example, N_2^+/N^+ in a nitrogen plasma.[17] Since there is no mass separation in a PIII machine, all ions in the plasma are implanted, and the depth profile is broadened because each N atom in N_2^+ is implanted with half of the total energy. Assuming that the ratio of $N_2^+:N^+ = \eta:(1-\eta)$, the fraction of the incident atoms with energy between W_1 and W_2 is

$0 \leq W < 0.5 e V_0$ (from N_2^+/N^+ plasma),

$$\delta_{a,W_1,W_2} = 0.7368 \times \frac{(W_2^{5/6} - W_1^{5/6}) \times (2.5636 \times \eta + 1)}{(x-0.6)^{1/3} \times (\eta + 1)}, \tag{15}$$

$0.5 e V_0 \leq W < e V_0$ (from N^+ plasma),

$$\delta_{a,W_1,W_2} = 0.7368 \times \frac{(W_2^{5/6} - W_1^{5/6}) \times (1-\eta)}{(x-0.6)^{1/3} \times (1+\eta)}. \tag{16}$$

The fraction of the incident atoms with energy $W = 0.5 e V_0$ from N_2^+ is

$$\delta_{a1} = [1 - 0.7368 \times (x-0.6)^{-1/3}] \times 2 \times \eta/(1+\eta), \tag{17}$$

$W = e V_0$

$$\delta_a = [1 - 0.7368 \times (x-0.6)^{-1/3}] \times \frac{(1-\eta)}{(1+\eta)}. \tag{18}$$

III. DISCUSSION

Based on Child–Langmuir law and a typical wave form such as that displayed in Fig. 2, we can conveniently ignore the effect of the fall time of the voltage pulse to derive a handy numerical description of the energy distribution of the incident particles (including ions and atoms resulting from molecular ions). Figure 3 depicts the effects of neglecting the fall time on the total ion dose difference. The maximum difference occurs at $t_p = 0.0$ and is about 21%, but this triangular wave form consisting only of rise and fall times in a single pulse has very little applications. When the plateau voltage duration is equal to rise time, the difference decreases to 8% and less than 1% for $t_w/t_r = 14$ (2 μs rise time and 28 μs pulse duration which are typical experimental parameters). Thus, omitting the fall time in the calculation of the energy distribution is quite reasonable, since the error introduced is very small. Figure 4 shows the energy distribution as a function of the ratio of the rise time to the steady-state (plateau) duration. We also compare the results generated by our analytical model to those predicted by Stewart [Eq. (11)] with consideration of the fall time. The good correlation demonstrates that the approximations in our model are reasonable in spite of the small difference stemming from

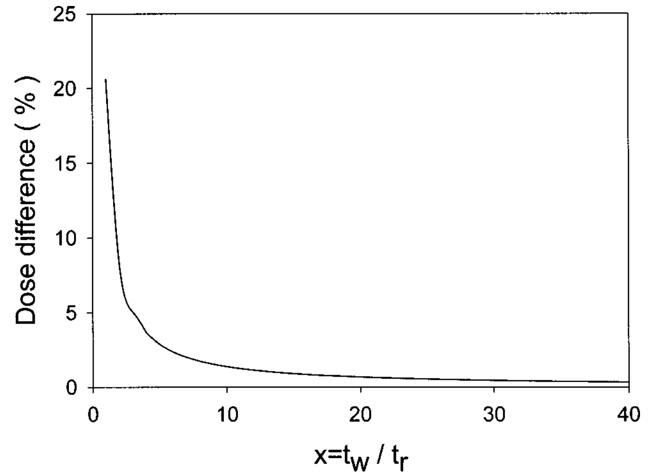

FIG. 3. Effects of the fall time of the voltage pulse on the total incident dose difference ($t_r = t_f$).

the fall time, and that our assumption that the number of ions implanted during the fall time of the voltage pulse is small, is indeed valid. By omitting the fall time, a simple and effective analytical model can be derived to predict the energy distribution of the incidental particles including both atomic and molecular ions.

As expected, the number of low-energy ions increases with a longer rise time and the trend is the same as that predicted by numerical simulation using the more complicated plasma fluid model.[18,19] In fact, the results of the fluid and our models are quite consistent for a low value of W_{min}/V_0, although the difference becomes bigger at larger W_{min}/V_0. This discrepancy may be attributed to the approximation that the sheath remains constant while an ion entering the sheath flies towards the target. Our simple model may underestimate slightly the fraction of the ions with high W_{min}.

As shown in Fig. 2, a large portion of the ions is implanted in the early stage (rise time duration) of the voltage pulse, as indicated by the initial high current. Even if we

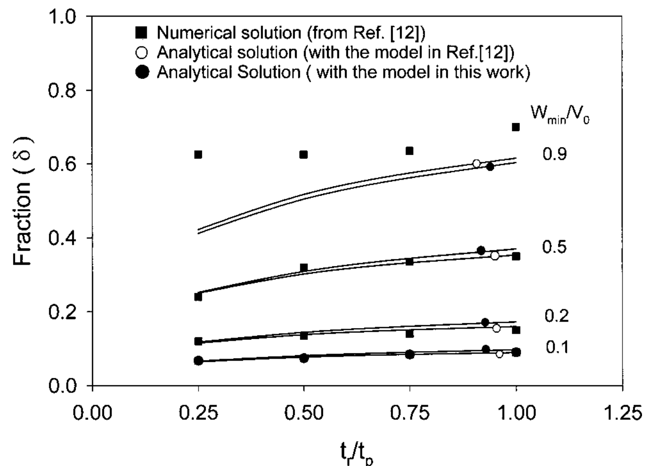

FIG. 4. Ion fractions impacting the target with energies $W < W_{min}$ vs $t_r/t_p (t_r + t_p = 1)$ for various W_{min}/V_0 ratios. The results derived by our model agree well with those obtained by a more complicated model described in Ref. 12.

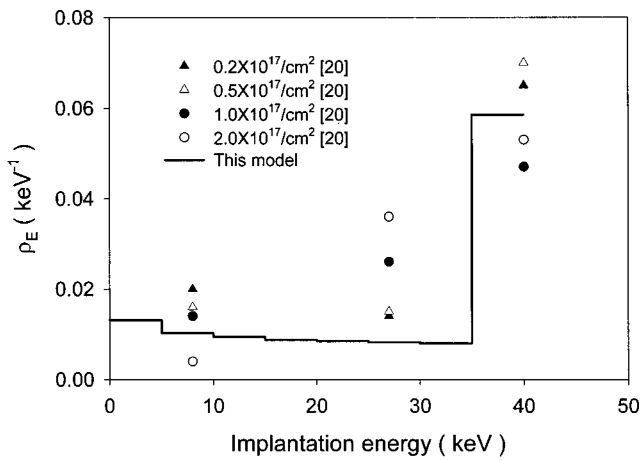

FIG. 5. Comparison of the energy distribution derived by our model with experimental results described in Ref. 20.

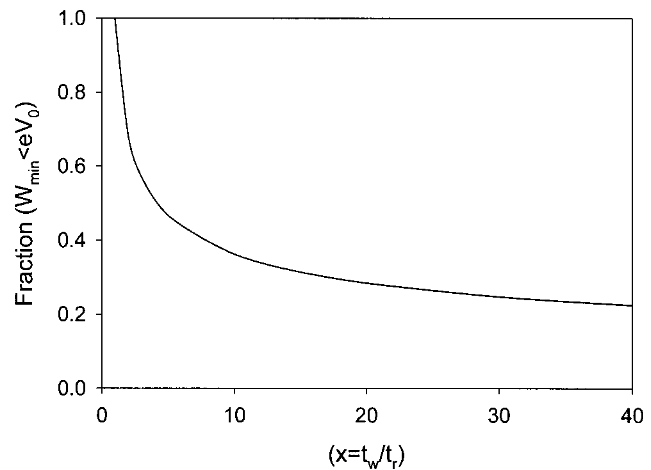

FIG. 6. Fraction of the ions hitting the target with energies $W<eV_0$ vs t_w/t_r.

eliminate the effects of the displacement current, the effective current is still very big.[16] Thus, the incident ions inherently carry different energies and the energy spectrum depends on the voltage wave form. From Eq. (8), the energy distribution of the incident ions is exclusively determined by the ratio of the pulse duration to the rise time and independent of the implantation voltage, plasma composition, and ion species. Thus, unified analytical expressions can accommodate various plasma conditions. For instance, the ion energy spectra of different ion species can be directly compared.

Equations (8) and (9) are simple equations that can be used to conveniently predict the energy distribution in practical PIII experiments. Experimentally, several related investigations have been conducted.[20–24] For example, for $t_w = 10\ \mu\text{s}/t_r = 6\ \mu\text{s}$ and $t_w = 21\ \mu\text{s}/t_r = 8.5\ \mu\text{s}$, the percentages of ions impacting the target with full energy calculated by our model is 27.9% and 40.2%, respectively. The results are consistent with the numerical simulation results (30% and 40%) based on a fluid model.[25] This confirms the validity of our simple model. In addition, as indicated in Fig. 5, the discrete energy distribution derived from our model shows good agreement with experimental results published in Refs. 20 and 21, particularly for the samples implanted with low-incident doses. In their experiments, the samples were implanted using $t_w = 2.5\ \mu\text{s}$ and $t_r = 1\ \mu\text{s}$. However, it should be noted that the discrepancy between the experimental results in Refs. 20 and 24 and the model is larger at high-incident doses. It is believed to be related to the formation of silicon oxide[20] or nitride[24] in the top layer as well as the validity of numerical fits with TRIM code at higher doses. With the formation of surface oxide or nitride, the electrical potential on the silicon sample will decrease and, consequently, the average incident ion energy is smaller, leading to an increase in the ion fraction with medium energies. Hence, the ion fraction with medium energy goes up and that with full energy decreases with increasing energy for doses beyond $1.0\times10^{17}\ \text{cm}^{-2}$.[20,24] The implantation parameters described in Ref. 20 (pulse duration, plasma density, voltage, and working pressure) favor the model. For instance, the plasma sheath is more planar due to a short duration and resulting thin sheath, the voltage is constant during the small ion transit time through the sheath, and the incident ions do not collide with other particles. On the contrary, the sheath described in Ref. 24 is much thicker. The longer ion transit time through the sheath on account of the higher voltage and lower plasma density increases the probability of collisions and decreases the acceleration energy due to sheath expansion. It should be noted that this and other models[12] do not take into account the collision effects, which can lead to significantly different results such as the results obtained at a high working gas pressure (5.0×10^{-2} Torr) described in Ref. 22. The energy distribution thus depends on the particle density or pressure through the ion mean-free path. For a sheath thickness larger than the mean-free path, the ions will undergo collisions before implantation, and their energy will be reduced.[22,26]

Figure 6 shows the fraction of ions possessing an energy less than eV_0 as a function of the ratio of the pulse duration to the rise time. The rise time has a more pronounced effect on the ion energy distribution than the plateau duration. A pulse duration of 40 μs consisting of a 1 μs rise time results in at most 80% of the implanted ions obtaining the full energy. In contrast, if $t_w = 40\ \mu\text{s}$ and $t_r = 4\ \mu\text{s}$ (that is, adding 3 μs to the rise time), the ratio decreases to about 60%, but if the same 3 μs are added to the pulse duration making $t_w = 43\ \mu\text{s}$ and $t_r = 1\ \mu\text{s}$, the ratio is hardly changed from 80%. The results reiterate the importance of a small rise time to achieve monoenergetic implantation. This characteristic can be exploited in practical situations. If a process calls for implanting a given dose at a given energy distribution, it may be more convenient to adjust the rise time than to change the total pulse duration.

Prior knowledge of the energy spectra of the incident ions is of great importance when designing PIII experiments, and so a simple analytical model such as the one presented in this article is very useful to process engineers. Figure 7 shows the effects of the pulse duration on the ion energy spectra. The energy spectra are characterized by high- and low-energy components. It should be noted that the ions with the lower energy are due to the small initial expanding

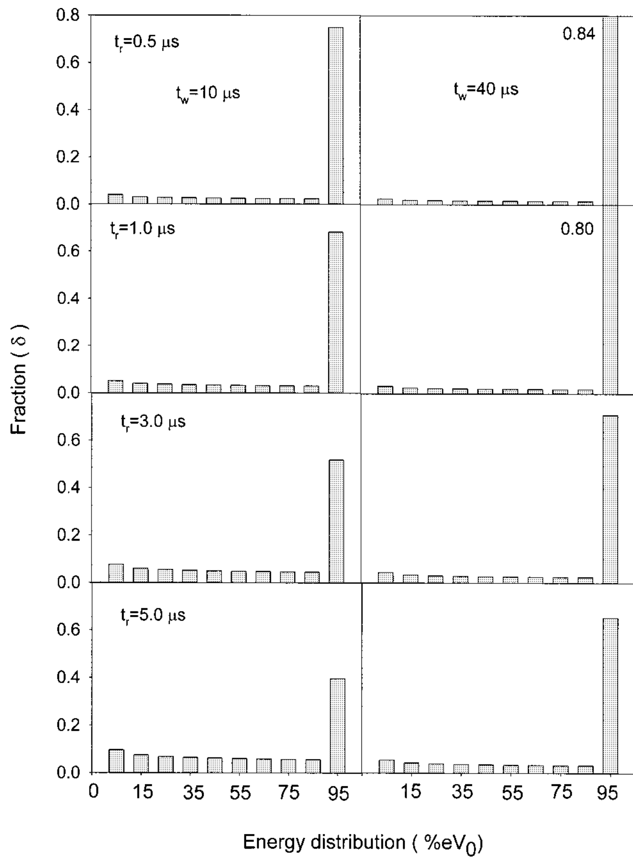

FIG. 7. Ion energy spectra for different rise times for pulse durations of 10 or 40 μs.

sheath obeying the Child–Langmuir law. To further illustrate the versatility and simplicity of our model, Fig. 8 depicts the derived energy distribution for a nitrogen PIII experiment in which both the monomer (N^+) and dimer (N_2^+) exist in the plasma. In this case, the low-energy component results in a smaller implantation depth for these ions and more severe sputtering effects. It also makes the in-depth distribution

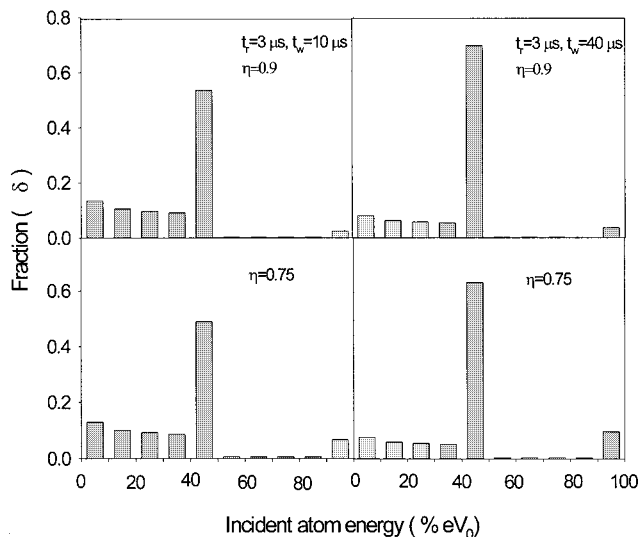

FIG. 8. Ion fractions for different t_w for two gas compositions $[N_2^+:N^+ = \eta:(1-\eta)]$.

more non-Gaussian.[20,21,24,27] Based on our model, for a higher ratio of the atomic ions (from $\eta=0.9$ to $\eta=0.75$), the atoms possessing the full energy increase from 3.6% to 9.7% for an implantation pulse duration of 40 μs and rise time of 3 μs. Such information can easily be obtained by our model without tedious trial-and-error experiments.

IV. CONCLUSION

The rise time of the high-voltage pulse is finite during PIII due to the equivalent capacitance effects of the PIII hardware and plasmas. Consequently, even under collisionless conditions, the ion energy is not unique. We have established a simple and effective model to calculate the energy distribution for easier control and optimization of the PIII process. More importantly, our model shows that the implantation energy is influenced significantly only by the ratio of the pulse duration to the rise time but independent of other parameters such as the implantation voltage, plasma composition, and ion species. Not only can the calculation be simplified significantly, direct comparison among different plasma conditions, for example, different ion species, can be performed directly. Our results also show that a long pulse duration does not increase the fraction of ions with the full acceleration energy significantly, whereas a small rise time yields a more appreciable effect. Therefore, in order to accomplish monoenergetic implantation, priority must be given to minimize the capacitance effects of the PIII hardware.

ACKNOWLEDGMENTS

The work was supported by Hong Kong RGC Earmarked Grant Nos. 9040344 and 9040412, Hong Kong RGC/Germany Joint Scheme Nos. 9050084 and 9050150, as well as City University of Hong Kong Strategic Research Grant No. 7001028.

[1] J. M. Mayer, L. Eriksson, and J. A. Davies, *Ion Implantation in Semiconductors* (Academic, London, 1970).
[2] J. F. Ziegler, *Handbook of Ion Implantation Technology* (North-Holland, Amsterdam, 1992).
[3] J. R. Conrad, J. L. Radtke, R. A. Dodd, F. J. Worzala, and N. C. Tran, J. Appl. Phys. **62**, 4591 (1987).
[4] P. K. Chu, S. Qin, C. Chan, N. W. Cheung, and L. A. Larson, Mater. Sci. Eng., R. **17**, 207 (1996).
[5] D. Z. Wang, T. C. Ma, and Y. Gong, J. Appl. Phys. **73**, 4171 (1993).
[6] M. Paulus, L. Stals, U. Rude, and B. Rauschenbach, J. Appl. Phys. **85**, 761 (1999).
[7] T. E. Sheridan, D. T. K. Kwok, and P. K. Chu, Appl. Phys. Lett. **72**, 1286 (1998).
[8] M. A. Lieberman, J. Appl. Phys. **66**, 2926 (1989).
[9] D. T. K. Kwok, P. K. Chu, B. P. Wood, and C. Chan, J. Appl. Phys. **86**, 1817 (1999).
[10] D. T. K. Kwok, X. C. Zeng, Q. C. Chen, P. K. Chu, and T. E. Sheridan, IEEE Trans. Plasma Sci. **27**, 225 (1999).
[11] R. R. Speth, G. A. Emmert, and M. J. Goeckner, Appl. Phys. Lett. **65**, 2272 (1994).
[12] R. A. Stewart and M. A. Lieberman, J. Appl. Phys. **70**, 3481 (1991).
[13] S. Qin and C. Chan, IEEE Trans. Plasma Sci. **20**, 569 (1992).
[14] P. K. Chu, B. Y. Tang, Y. C. Cheng, and P. K. Ko, Rev. Sci. Instrum. **68**, 1886 (1997).
[15] M. P. J. Gaudreau, J. A. Casey, M. A. Kempkes, T. J. Hawkey, and J. M. Mulvaney, J. Vac. Sci. Technol. B **17**, 888 (1999).
[16] X. B. Tian, B. Y. Tang, and P. K. Chu, J. Appl. Phys. **86**, 3567 (1999).
[17] B. Y. Tang, R. P. Fetherston, M. Shamim, R. A. Breun, A. Chen, and J. R. Conrad, J. Appl. Phys. **73**, 4176 (1993).

[18] G. A. Emmert, *IEEE International Conference on Plasma Science*, Oakland, CA, 21–23 May (IEEE, New York, 1990).
[19] G. A. Emmert and M. A. Henry, J. Appl. Phys. **71**, 113 (1992).
[20] N. P. Barradas, A. J. H. Maas, S. Mändl, and R. Günzel, Surf. Coat. Technol. **93**, 238 (1997).
[21] N. P. Barradas, A. J. H. Maas, S. Mändl, and R. Günzel, J. Appl. Phys. **81**, 6642 (1997).
[22] S. Qin, C. Chan, and N. E. McGruer, Plasma Sources Sci. Technol. **1**, 1 (1992).
[23] S. Mändl, R. Günzel, W. Möller, and J. Brutscher, Surf. Coat. Technol. **93**, 234 (1997).
[24] J. J. Vajo, J. D. Williams, R. Wei, R. G. Wilson, and J. N. Matossian, J. Appl. Phys. **76**, 5666 (1994).
[25] M. M. Shamim, D. E. Muller, K. Sridharan, R. P. Fetherston, N. Tran, and J. R. Conrad, J. Appl. Phys. **77**, 1015 (1995).
[26] D. Z. Wang, T. C. Ma, and X. L. Deng, J. Appl. Phys. **75**, 1335 (1994).
[27] P. K. Chu, X. Lu, S. S. K. Iyer, and N. W. Cheung, Solid State Technol. **40**, S9 (1997).